

Equation of state of asymmetric nuclear matter and the tidal deformability of neutron star

Ngo Hai Tan^{1,2}, Dao T. Khoa³, and Doan Thi Loan³

¹ Faculty of Fundamental Sciences, Phenikaa University, Hanoi 12116, Vietnam

² Phenikaa Institute for Advanced Study (PIAS), Phenikaa University, Hanoi 12116, Vietnam

³ Institute for Nuclear Science and Technology, VINATOM, Hanoi 100000, Vietnam

Received: date / Revised version: date

Abstract. Neutron star (NS) is a unique astronomical compact object where the four fundamental interactions have been revealed from the observation and studied in different ways. While the macroscopic properties of NS like mass and radius can be determined within the General Relativity using a realistic equation of state (EOS) of NS matter, such an EOS is usually generated by a nuclear structure model like, e.g., the nuclear mean-field approach to asymmetric nuclear matter. Given the radius of NS extended to above 10 km and its mass up to twice the solar mass, NS is expected to be tidally deformed when it is embedded in a strong tidal field. Such a tidal effect was confirmed unambiguously in the gravitation wave signals detected recently by the LIGO and Virgo laser interferometers from GW170817, the first ever direct observation of a binary NS merger. A nonrelativistic mean-field study is carried out in the present work within the Hartree-Fock formalism to construct the EOS of NS matter, which is then used to determine the tidal deformability, gravitational mass, and radius of NS. The mean-field results are compared with the constraints imposed for these quantities by the global analysis of the observed GW170817 data, and a strong impact by the incompressibility of nuclear matter on the hydrostatic configuration of NS is shown.

PACS. 21.65.+f Nuclear matter – 26.60.+c Nuclear matter aspects of neutron stars – 04.30.Tv Gravitational-wave astrophysics

1 Introduction

Neutron star (NS) is an astronomical compact object consisting of the lepton and baryon matter under the extreme conditions, and it has been therefore a long standing research object of the modern nuclear physics and nuclear astrophysics. The equation of state (EOS) of high-density nuclear matter (NM) in the NS core is the main synergy between nuclear physics and astrophysics. Using a realistic EOS of asymmetric NM characterized by a large neutron excess, the General Relativity not only explains the compact shape of NS in the hydrostatic equilibrium with its maximum mass limited to about twice the solar mass, but also predicts the interesting behavior of NS in the presence of a strong gravitational field. In particular, the shape of NS is tidally deformed to gain a nonzero quadrupole moment under the gravitational field formed by the mutual attraction of two coalescing neutron stars [1, 2]. The gravitational wave (GW) emitting from such a binary NS merger has been expected to be detectable by the GW observatories on Earth. Although some indirect evidences of the NS merger were suggested earlier, the first direct observation of a binary NS merger has been reported on August 17, 2017, with the GW signals detected by LIGO and Virgo laser interferometers [3], and the γ ray burst

detected by the Fermi γ ray space telescope [4]. This exciting event is now widely referred to as GW170817, which opened a new era of the multimessenger astronomy.

The GW and γ ray burst emitted from GW170817, as well as the x ray, infrared radiations, and visible light detected later by more than 70 telescopes provide a huge database for the nuclear physics and astrophysics research. By analyzing the observed GW signals from GW170817 [5], the tidal deformability of NS has been determined and translated into a constraint for the gravitational mass and radius of NS. This result soon became an important reference for numerous nuclear physics studies of NS, and further constraints for the EOS of NM and hydrostatic configuration of NS have been suggested [6–10].

A realistic EOS of NS matter (the dependence of the pressure of NS matter on the mass-energy density) is the key input for the determination of the macroscopic properties of NS like gravitational mass, radius, inertia moment and tidal deformability. For this purpose, a nonrelativistic mean-field study of the EOS of NM within the Hartree-Fock (HF) formalism has been done in the present work, using several versions of the (in-medium) density dependent nucleon-nucleon (NN) interaction [11, 12]. Using the EOS of asymmetric NM obtained from the HF calculation, the $n\rho e\mu$ matter of the uniform NS core is generated

from the charge neutrality and lepton number conservation implied by the β equilibrium. The EOS of the $npe\mu$ matter is then used to determine the tidal deformability, gravitational mass and radius of NS, and a detailed comparison with the constraints imposed for these quantities by the GW170817 observation is made.

2 Hartree-Fock formalism for the EOS of nuclear matter

The nonrelativistic HF method [11] is used in the present work to model the EOS of asymmetric NM at zero temperature, which is characterized by the neutron and proton number densities, n_n and n_p , or equivalently by the total baryon number density $n_b = n_n + n_p$ and neutron-proton asymmetry $\delta = (n_n - n_p)/n_b$. The total HF energy density of NM is obtained as

$$\mathcal{E} = \mathcal{E}_{\text{kin}} + \frac{1}{2} \sum_{\mathbf{k}\sigma\tau} \sum_{\mathbf{k}'\sigma'\tau'} [\langle \mathbf{k}\sigma\tau, \mathbf{k}'\sigma'\tau' | v_d | \mathbf{k}\sigma\tau, \mathbf{k}'\sigma'\tau' \rangle + \langle \mathbf{k}\sigma\tau, \mathbf{k}'\sigma'\tau' | v_{\text{ex}} | \mathbf{k}'\sigma\tau, \mathbf{k}\sigma'\tau' \rangle], \quad (1)$$

where $|\mathbf{k}\sigma\tau\rangle$ are plane waves, v_d and v_{ex} are the direct and exchange terms of the in-medium NN interaction.

We have chosen for the present mean-field study several versions of the density dependent NN interaction based on the G-matrix M3Y interaction [13], which were used successfully in the HF studies of NM [11,12] and the folding model analysis of the nucleus-nucleus scattering [14,15]. Explicitly, the density dependent NN interaction is just the original M3Y interaction supplemented by a realistic density dependence

$$v_{d(\text{ex})}(n_b, r) = F_{00}(n_b)v_{00}^{d(\text{ex})}(r) + F_{10}(n_b)v_{10}^{d(\text{ex})}(r)(\boldsymbol{\sigma}\boldsymbol{\sigma}') + F_{01}(n_b)v_{01}^{d(\text{ex})}(r)(\boldsymbol{\tau}\boldsymbol{\tau}') + F_{11}(n_b)v_{11}^{d(\text{ex})}(r)(\boldsymbol{\sigma}\boldsymbol{\sigma}')(\boldsymbol{\tau}\boldsymbol{\tau}'). \quad (2)$$

We consider in the present work the *spin-saturated* NM, so that the σ -components of plane waves are averaged out in the HF calculation (1), and only the v_{00} and v_{01} terms of the central interaction (2) are necessary for the determination of the energy density of NM. The radial parts of the central interaction (2) are determined from the spin singlet and triplet components of the M3Y interaction [13], and expressed in terms of three Yukawa functions [16] as

$$v_{00(01)}^{d(\text{ex})}(r) = \sum_{\kappa=1}^3 Y_{00(01)}^{d(\text{ex})}(\kappa) \frac{\exp(-R_\kappa r)}{R_\kappa r}, \quad (3)$$

with the Yukawa strengths given explicitly in Table 1. Originally, the *isoscalar* density dependence $F_{00}(n_b)$ was parametrized in Ref. [14] to correctly reproduce the saturation properties of symmetric NM at the saturation baryon density $n_0 \approx 0.17 \text{ fm}^{-3}$. About 20 years after, the *isovector* density dependence $F_{01}(n_b)$ was parametrized to reproduce the microscopic Brueckner-Hartree-Fock results of asymmetric NM, with the total strength slightly

Table 1. Yukawa strengths of the M3Y interaction [13].

κ	R_κ (fm^{-1})	$Y_{00}^d(\kappa)$ (MeV)	$Y_{01}^d(\kappa)$ (MeV)	$Y_{00}^{\text{ex}}(\kappa)$ (MeV)	$Y_{01}^{\text{ex}}(\kappa)$ (MeV)
1	4.0	11061.625	313.625	-1524.25	-4118.0
2	2.5	-2537.5	223.5	-518.75	1054.75
3	0.7072	0.0	0.0	-7.8474	2.6157

adjusted by the folding model description of the charge exchange (p, n) reaction to the isobar analog states in finite nuclei [17,18]. Note that the CDM3Y8 version of the density dependent NN interaction has been parametrized recently in the mean-field study of the spin-polarized NS matter [19], including the density dependence of the spin- and spin-isospin terms of the interaction (2). Thus, the following density dependent functional is used for the interaction (2)

$$F_{st}(n_b) = C_{st} [1 + \alpha_{st} \exp(-\beta_{st} n_b) + \gamma_{st} n_b], \quad (4)$$

and all the parameters are given explicitly in Table 2. The parameters of $F_{00}(n_b)$ of the CDM3Y8 version are slightly fine tuned in the present study to reproduce the same binding energy $E_0 \approx 15.8 \text{ MeV}$ at the saturation density $n_0 \approx 0.17 \text{ fm}^{-3}$ as those obtained with the other 5 versions of the density dependent NN interaction that were originally parametrized in Ref. [14]. The parameters of $F_{01}(n_b)$ of all 6 versions are also readjusted in the present work to reduce the uncertainty at high baryon densities, and to reach a better agreement of $E_{\text{sym}}(n_b)$ given by the HF calculation with the ab-initio results [20,21] at $n_b > n_0$. The total HF energy density (1) of the asymmetric NM is then obtained as

$$\mathcal{E} = \frac{3\hbar^2}{10m} [k_{F_n}^2 n_n + k_{F_p}^2 n_p] + F_{00}(n_b)\mathcal{E}_{00} + F_{01}(n_b)\mathcal{E}_{01}, \quad (5)$$

where m is the nucleon mass, and the potential energy density of NM is determined with

$$\mathcal{E}_{00} = \frac{1}{2} \left[n_b^2 J_{00}^d + \int A_{00}^2 v_{00}^{\text{ex}}(r) d^3 r \right],$$

$$\mathcal{E}_{01} = \frac{1}{2} \left[n_b^2 J_{01}^d \delta^2 + \int A_{01}^2 v_{01}^{\text{ex}}(r) d^3 r \right]. \quad (6)$$

Here $J_{00(01)}^d = \int v_{00(01)}^d(r) d^3 r$ is the volume integral of the direct interaction, and the exchange integrals are evaluated with

$$A_{00(01)} = n_n \widehat{j}_1(k_{F_n} r) \pm n_p \widehat{j}_1(k_{F_p} r), \quad (7)$$

where $\widehat{j}_1(x) = 3j_1(x)/x$, and $j_1(x)$ is the first-order spherical Bessel function. The nucleon Fermi momentum is determined as $k_{F_{n(p)}} = [3\pi^2 n_{n(p)}]^{1/3}$. One can see that the nonzero neutron-proton asymmetry ($\delta \neq 0$ or $n_n \neq n_p$) results on a nonzero contribution from \mathcal{E}_{01} term to the total NM energy density (5), which is the case for both the crust and core of NS.

Table 2. Parameters of 6 versions of the density dependent NN interaction (2)-(4) used in the present HF calculation. The parameters of $F_{00}(n_b)$ were adjusted to reproduce the binding energy $E_0 \approx 15.8$ MeV and different values of the nuclear incompressibility K of symmetric NM at the saturation density $n_0 \approx 0.17$ fm $^{-3}$. The parameters of $F_{01}(n_b)$ were fine tuned to give $E_{\text{sym}}(n_0) \approx 30$ MeV and $L \approx 50$ MeV at n_0 , and a good agreement of the calculated $E_{\text{sym}}(n_b)$ with the ab-initio results [20,21] at higher densities.

Interaction	C_{00}	α_{00}	β_{00} (fm 3)	γ_{00} (fm 3)	C_{01}	α_{01}	β_{01} (fm 3)	γ_{01} (fm 3)	K (MeV)
CDM3Y3	0.2985	3.4528	2.6388	-1.5	0.2342	5.3336	6.4738	4.3172	217
CDM3Y4	0.3052	3.2998	2.3180	-2.0	0.2129	6.3581	7.0584	5.6091	228
CDM3Y5	0.2728	3.7367	1.8294	-3.0	0.2204	6.6146	7.9910	6.0040	241
CDM3Y6	0.2658	3.8033	1.4099	-4.0	0.2313	6.6865	8.6775	6.0182	252
CDM3Y8	0.2658	3.8033	1.3035	-4.3	0.2643	6.3836	9.8950	5.4249	257
BDM3Y1	1.2521	0.0	0.0	-1.7452	0.2528	7.6996	11.0386	6.3568	270

Dividing the total NM energy density (5) by the baryon number density, we obtain the NM energy per baryon E/A which can be expanded over the neutron-proton asymmetry δ as

$$\frac{\mathcal{E}}{n_b} \equiv \frac{E}{A}(n_b, \delta) = \frac{E}{A}(n_b, \delta = 0) + E_{\text{sym}}(n_b)\delta^2 + O(\delta^4) + \dots, \quad (8)$$

where $E_{\text{sym}}(n_b)$ is the **nuclear symmetry energy**. The contribution from $O(\delta^4)$ and higher-order terms in Eq. (8) is proven to be small and can be neglected in the *parabolic* approximation [16], where $E_{\text{sym}}(n_b)$ equals the energy required per baryon to change the symmetric NM (with $\delta = 0$) to the pure neutron matter (with $\delta = 1$). Thus, the two key quantities characterizing EOS of NM are the energy of symmetric NM and nuclear symmetry energy. At the saturation density $n_0 \approx 0.17$ fm $^{-3}$, these two quantities are constrained by the empirical values inferred from the structure studies of finite nuclei

$$E_0 = \frac{E}{A}(n_0, \delta = 0) \approx -15.8 \text{ MeV}, \quad E_{\text{sym}}(n_0) \approx 30 \text{ MeV}.$$

However, their behavior at higher baryon densities of NM ($n_b > n_0$) remains less certain because of the difficulties for the terrestrial nuclear physics experiments to access the high-density NM. The pressure of baryon matter inside the high-density medium of NS is determined as

$$P(n_b, \delta) = n_b^2 \frac{\partial}{\partial n_b} \left[\frac{E}{A}(n_b, \delta) \right] = P(n_b, \delta = 0) + P_{\text{sym}}(n_b)\delta^2 + O(\delta^4) + \dots, \quad (9)$$

which is expanded over δ in the same parabolic approximation [16] as in Eq. (8). The total energy of symmetric NM and nuclear symmetry energy at high baryon densities correlate strongly with the nuclear incompressibility K and slope parameter of the symmetry energy L , respectively, determined at the saturation density as

$$K = 9 \frac{\partial P(n_b, \delta = 0)}{\partial n_b} \Big|_{n_b \rightarrow n_0}, \quad L = 3n_b \frac{\partial E_{\text{sym}}(n_b)}{\partial n_b} \Big|_{n_b \rightarrow n_0}. \quad (10)$$

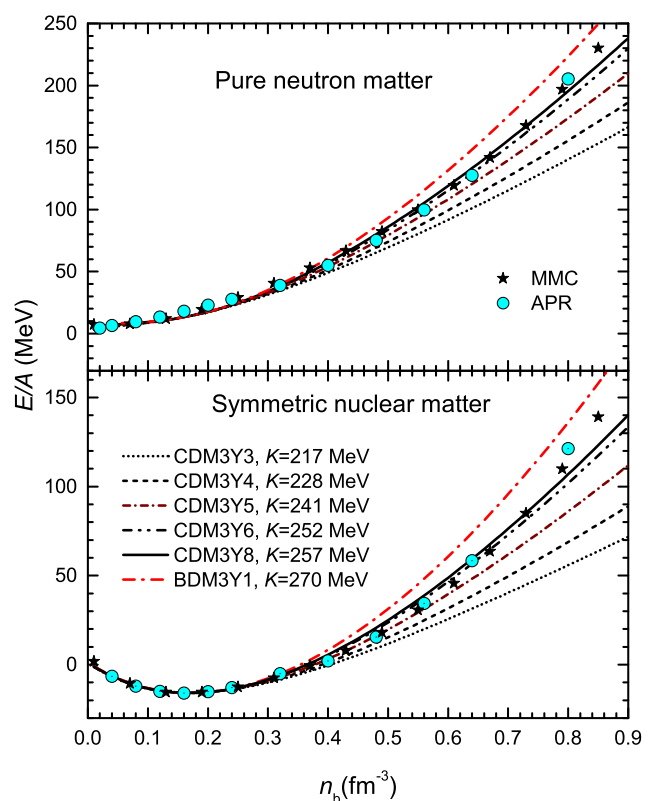


Fig. 1. The energy per baryon of symmetric NM (lower panel) and pure neutron matter (upper panel) given by the HF calculation, using 6 versions of the density dependent NN interaction (2)-(4). The circles and stars are the results of the ab-initio calculation by Akmal, Pandharipande and Ravenhall (APR) [20] and microscopic Monte Carlo (MMC) calculation by Gandolfi *et al.* [21], respectively. K is the nuclear incompressibility (10) of symmetric NM at the saturation density $n_0 \approx 0.17$ fm $^{-3}$.

The K and L values are strongly sensitive to the EOS of NM. The compressibility K has been a key research topic of numerous structure studies of nuclear monopole excitation (see, e.g., Ref. [22] and references therein) as well as studies of the heavy-ion (HI) collisions [23] and nucleus-nucleus scattering [24]. These researches have pinned down this quantity to $K \approx 240 \pm 20$ MeV. The present HF calcu-

lation (10) of NM using 6 different versions of the density dependent NN interactions (2)-(4) tabulated in Table 2 gives $K \approx 217 - 270$ MeV, which agree well with the empirical value.

The HF results for the energy per baryon of symmetric NM and pure neutron matter and are plotted in Fig. 1, in comparison with the *ab-initio* results of the many-body variational calculation by Akmal *et al.* [20] using the Argonne-AV18 NN potential, and microscopic Monte Carlo calculation of NM by Gandolfi *et al.* [21] using the Argonne-AV6' NN potential supplemented by an empirical density dependence. The sensitivity of the EOS to the K value is well illustrated in Fig. 1, and the HF results given by the CDM3Y6 and CDM3Y8 interactions (associated with $K \approx 252$ and 257 MeV, respectively) agree nicely with the *ab-initio* results [20,21] at high baryon densities. The effect caused by the difference in the K values shows up also in the macroscopic properties of NS (see the discussion below in Sec. 4).

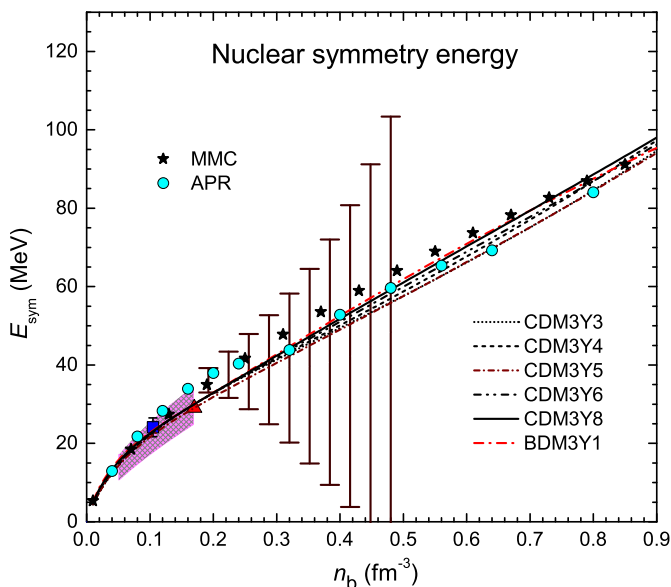


Fig. 2. The nuclear symmetry energy $E_{\text{sym}}(n_b)$ given by the HF calculation using 6 versions of the density dependent NN interaction (2)-(4). The shaded region is the range constrained by the HI data [25,26], the square and triangle are values suggested by the structure studies [27–29]. The vertical bars are the empirical range obtained at the 90% confidence level from the Bayesian analysis [31] of the NS radius $R_{1/4}$ versus the GW170817 constraint [5]. The same denotations as in Fig. 1 for the circles and stars.

At variance with the nuclear incompressibility K that helps to constrain the behavior of the EOS of symmetric NM at high densities, it is more difficult to constrain the density dependence of the nuclear symmetry energy E_{sym} at densities $n_b > n_0$. In fact, E_{sym} has been well constrained at low baryon densities by the (isospin dependent) data of the HI fragmentation [25,26], and by the

structure studies of the giant dipole resonances [27], neutron skins [28,29], and nuclear mass differences [30]. The HF results for E_{sym} at low baryon densities agree well with the empirical data (see Fig. 2). The behavior of the nuclear symmetry energy at higher baryon densities ($n_b > n_0$) remains poorly known. One can see in Fig. 2 that the HF results obtained for E_{sym} at $n_b > n_0$ with the revised isovector density dependence of the interaction agree well with the *ab-initio* results [20,21], and the slope parameter of the nuclear symmetry energy $L \approx 50$ MeV is obtained with all 6 versions of the density dependent NN interaction (see Table 2). Recently, the symmetry energy at baryon densities up to $3n_0$ was inferred from the Bayesian analysis of the correlation of different EOS's of $npe\mu$ matter and the predicted radius $R_{1/4}$ of NS with mass $M = 1.4 M_\odot$ versus the GW170817 constraint imposed by the tidal deformability of NS. The empirical E_{sym} values suggested for baryon densities approaching $3n_0$ at the 90% confidence level [31] are shown as the vertical bars in Fig. 2, and the uncertainty still remains so large that the results of the HF and *ab-initio* calculations are all enclosed inside the empirical boundaries, over the whole range of baryon density.

3 β -stable $npe\mu$ matter of neutron star

The HF model (1) describes the ideal NM that contains nucleons only. In fact, the NS matter contains significant lepton fraction in both the crust and uniform core, and a realistic EOS of NS matter should include the lepton contribution. In the present work, we use the EOS of the NS crust obtained by Douchin *et al.* [32,33] in the Compress Liquid Drop Model based on the SLy4 interaction between nucleons [34], with fully ionized atoms and a degenerate Fermi gas of free electrons. At the edge density $n_{\text{edge}} \approx 0.076 \text{ fm}^{-3}$, a weak first-order phase transition takes place between the NS crust and uniform core of NS [32]. At baryon densities $n_b \gtrsim n_{\text{edge}}$ the core of NS is described as a homogeneous matter of neutrons, protons, electrons and negative muons (μ^- appear at n_b above the muon threshold density $\mu_e > m_\mu c^2 \approx 105.6$ MeV). The total mass-energy density \mathcal{E} of the $npe\mu$ matter inside NS core is determined as

$$\mathcal{E}(n_n, n_p, n_e, n_\mu) = \mathcal{E}_{\text{HF}}(n_n, n_p) + n_n m_n c^2 + n_p m_p c^2 + \mathcal{E}_e(n_e) + \mathcal{E}_\mu(n_\mu), \quad (11)$$

where $\mathcal{E}_{\text{HF}}(n_n, n_p)$ is the HF energy density (3) of asymmetric NM, \mathcal{E}_e and \mathcal{E}_μ are the energy densities of electrons and muons given by the relativistic Fermi gas model [35]. In such a Fermi gas model, the lepton number densities n_e and n_μ are determined from the charge neutrality condition ($n_p = n_e + n_\mu$), and the β -equilibrium of (neutrino-free) NS matter is sustained by the balance of the chemical potentials

$$\mu_n = \mu_p + \mu_e \quad \text{and} \quad \mu_e = \mu_\mu, \quad \text{where} \quad \mu_j = \frac{\partial \mathcal{E}_j}{\partial n_j}. \quad (12)$$

The fractions of the constituent particles in NS matter are determined at the given baryon density n_b as $x_j = n_j/n_b$. Below the muon threshold density ($\mu_e < m_\mu c^2 \approx 105.6$ MeV) the charge neutrality condition leads to the following relation [36]

$$3\pi^2(\hbar c)^3 n_b x_p - \hat{\mu}^3 = 0, \quad \text{where } \hat{\mu} = \mu_n - \mu_p = 2 \frac{\partial \mathcal{E}_{\text{HF}}}{\partial \delta}. \quad (13)$$

The density dependence of the proton fraction in the β -equilibrium, $x_p(n_b)$, can then be obtained from the solution of Eq. (13). If we assume the parabolic approximation and neglect the contribution from higher-order terms in (8), then $x_p(n_b)$ is given by the solution of the well-known equation [36]

$$3\pi^2(\hbar c)^3 n_b x_p - [4E_{\text{sym}}(n_b)(1 - 2x_p)]^3 = 0, \quad (14)$$

which shows the important role of the nuclear symmetry energy in the determination of the proton abundance in NS matter.

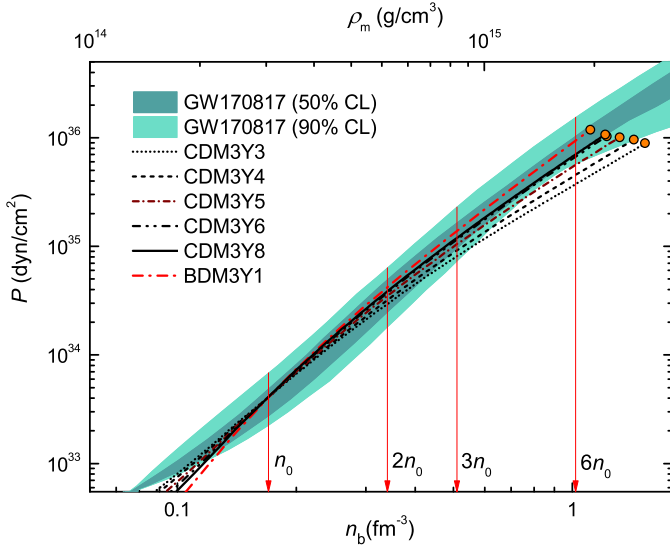


Fig. 3. The total pressure of NS matter (16) over the whole range of the rest-mass (ρ_m) and baryon-number (n_b) densities, given by the HF calculation (11)-(16) using 6 versions of the density dependent NN interaction (2)-(4). The dark and light shaded regions enclose the empirical pressure given by the “spectral” EOS inferred from the Bayesian analysis of the GW170817 data with the 50% and 90% confidence levels, respectively, keeping the lower limit of the maximum NS mass at $1.97 M_\odot$ [5]. The circles are the pressure $P(n_c)$ at the maximum central density n_c obtained with each interaction (see Table 3).

As baryon densities exceeding the muon threshold density, where $\mu_e > m_\mu c^2 \approx 105.6$ MeV, it is energetically favorable for electrons to convert to negative muons, and the charge neutrality condition leads to the relation [36]

$$3\pi^2(\hbar c)^3 n_b x_p - \hat{\mu}^3 - [\hat{\mu}^2 - (m_\mu c^2)^2]^{3/2} \theta(\hat{\mu} - m_\mu c^2) = 0, \quad (15)$$

where $\theta(x)$ is the Heaviside step function. Based on the solutions of Eqs. (11)-(15), the EOS of the β -stable $npe\mu$ matter is fully determined by the mass-energy density $\rho(n_b)$ and total pressure $P(n_b)$ of NS matter

$$\rho(n_b) = \mathcal{E}(n_b)/c^2, \quad P(n_b) = n_b^2 \frac{\partial}{\partial n_b} \left[\frac{\mathcal{E}_{\text{HF}}(n_b)}{n_b} \right] + P_e + P_\mu. \quad (16)$$

We show in Fig. 3 the total pressure of NS matter $P(n_b)$ given by the HF calculation using 6 versions of the density dependent NN interaction, over baryon densities up to above $6n_0$, in comparison with the empirical pressure given by the “spectral” EOS inferred from the Bayesian analysis of the GW170817 data at the 50% and 90% confidence levels [5]. In general, our mean-field results agree reasonably with the empirical pressure over baryon densities up to $3n_0$. The empirical pressure keeps steadily rising up at the highest densities in the center of NS, and this trend is due to the fact that sampling of the spectral EOS has been constrained [5] by the maximum NS mass $M_{\text{max}} \gtrsim 1.97 M_\odot$, based on the observation of the second PSR J0348 + 0432 with $M \approx 2.01 \pm 0.04 M_\odot$ [37]. Excepting the results obtained with the CDM3Y3 and CDM3Y4 interactions, the pressure of NS matter given by the other 4 versions of the density dependent NN interaction at high baryon densities follows closely the empirical trend up to the corresponding maximum central densities n_c (see Fig. 3 and Table 3). It is obvious that the lower pressure at high densities given by the CDM3Y3 and CDM3Y4 interactions is due to the smaller K values associated with these interactions. With the larger K values, the NS matter generated by the CDM3Y5, CDM3Y6, CDM3Y8 and BDM3Y1 interactions can be compressed to have higher pressure at high baryon densities, in agreement with the empirical pressure inferred from the GW170817 data. Because all 6 versions of the density dependent NN interaction were adjusted to obtain the same saturation energy $E_0 \approx 15.8$ MeV and $L \approx 50$ MeV at the saturation density n_0 , the NM pressure (9) is determined mainly by its symmetry term which is directly proportional to L , and the $P(n_0)$ values shown in Fig. 3 are nearly the same. At low baryon densities $n_b < n_0$, the slope of the energy of symmetric NM is opposite compared to that at $n_b > n_0$ (see Fig. 1), leading to the decrease of $P(n_b)$ with the increasing incompressibility K at subsaturation densities shown in Fig. 3.

Because the total pressure of NS matter is directly proportional to the total mass density, it is of interest to consider the *causality* condition [36] that implies the adiabatic sound velocity in the stellar medium to be *subluminal*

$$v_s = \sqrt{\frac{dP(\rho)}{d\rho}} < c, \quad (17)$$

where $P(\rho)$ is the total pressure of NS matter deduced from the relation (16) as function of the total mass density ρ . The sound velocity v_s given by the total pressure obtained with 6 versions of the density dependent NN interaction at different baryon number densities is shown in Fig. 4, and one can see that the causality condition

is well satisfied by the present EOS of NS matter. With about the same K values associated with the CDM3Y6 and CDM3Y8 interactions, these two versions of the interaction give more or less the same v_s values over the whole range of baryon density. The higher central pressure $P(\rho)$ associated with the higher nuclear incompressibility K corresponds also to the higher sound velocity. Given the recent discussion on the $c/\sqrt{3}$ bound of the sound velocity [38], it is complimentary to note that the EOS's obtained with the CDM3Y6, CDM3Y8, and BDM3Y1 interactions gives $v_s \gtrsim c/\sqrt{3}$ at baryon densities $n_b \gtrsim 3n_0$ where the corresponding pressures of NS matter also agree nicely with the empirical data [5] (see Fig. 3).

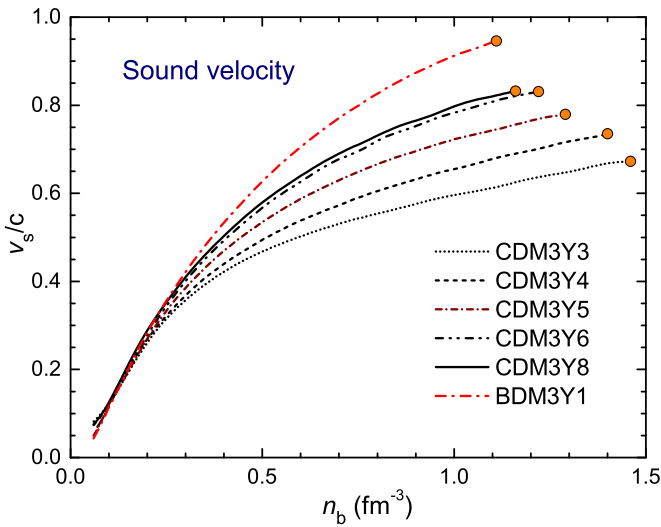


Fig. 4. The adiabatic sound velocity (17) in the NS medium given by 6 versions of the density dependent NN interaction (2)-(4). The circles are the v_s values obtained at the maximum central densities n_c with each interaction.

4 Tidal deformability, mass and radius of neutron star

An exciting effect observed by the GW170817 merger of two neutron stars is the tidal deformation of NS induced by the strong gravitational field, which enhances the GW emission and accelerates the decay of the quasicircular inspiral [5]. We give here a brief account of the tidal deformability of a static spherical star being in the hydrostatic equilibrium [1, 2]. If exposed to the gravitational field created by the attraction of the companion star in a binary system, this star is tidally deformed and gains a nonzero quadrupole moment Q_{ij} that is directly proportional to the field strength E_{ij}

$$Q_{ij} = -\lambda E_{ij}. \quad (18)$$

λ characterizes the star response to the gravitational field and is dubbed as the *tidal deformability* or quadrupole

polarizability of star. In the General Relativity, λ is related to the $l = 2$ tidal Love number k_2 [1] as

$$\lambda = \frac{2}{3G} k_2 R^5, \quad (19)$$

where R and G are the star radius and gravitational constant, respectively. For the discussion on the sensitivity to the EOS of NS matter, it is convenient to consider the dimensionless tidal deformability parameter Λ [5] expressed in terms of the compactness C of star with mass M and radius R as

$$\Lambda = \frac{2}{3} k_2 C^{-5}, \quad \text{with } C = \frac{GM}{Rc^2}. \quad (20)$$

Using the linearized Einstein equation, the Love number k_2 can be expressed [1, 2] as

$$\begin{aligned} k_2 = & \frac{8C^5}{5} (1 - 2C)^2 [2 + 2C(y - 1) - y] \\ & \times \{2C[6 - 3y + 3C(5y - 8)] \\ & + 4C^3[13 - 11y + C(3y - 2) + 2C^2(1 + y)] \\ & + 3(1 - 2C)^2 [2 - y + 2C(y - 1)] \ln(1 - 2C)\}, \end{aligned} \quad (21)$$

where $y = RH'(R)/H(R)$, and function $H(r)$ is related to the nonzero component of the metric perturbation of the stress-energy tensor. $H(r)$ and its radial derivative $H'(r)$ can be determined [1, 2] from the solution of the following differential equation

$$\begin{aligned} & H''(r) + H'(r) \left[1 - \frac{2GM(r)}{c^2 r} \right]^{-1} \left\{ \frac{2}{r} - \frac{2GM(r)}{c^2 r^2} \right. \\ & \left. - \frac{4\pi G}{c^4} r [\rho(r) - P(r)] \right\} + H(r) \left[1 - \frac{2GM(r)}{c^2 r} \right]^{-1} \\ & \left\{ \frac{4\pi G}{c^4} \left[5\rho(r) + 9P(r) + \frac{d\rho(r)}{dP(r)} (\rho(r) + P(r)) \right] - \frac{6}{r^2} \right. \\ & \left. - 4 \left[1 - \frac{2GM(r)}{c^2 r} \right]^{-1} \left[\frac{GM(r)}{c^2 r^2} + \frac{4\pi G}{c^4} r P(r) \right]^2 \right\} = 0. \end{aligned} \quad (22)$$

Here r is the radial coordinate in Schwarzschild metric, and $\mathcal{M}(r)$ is the gravitational mass enclosed within the sphere of radius r . $\rho(r)$ and $P(r)$ are the mass-energy density and pressure of star matter at radius r , respectively. In the present work, Eq. (22) is solved using the fourth-order Runge-Kutta method and integrated together with the Tolman-Oppenheimer-Volkoff (TOV) equations

$$\begin{aligned} \frac{dP(r)}{dr} = & -\frac{G\rho(r)\mathcal{M}(r)}{c^2 r^2} \left[1 + \frac{P(r)}{\rho(r)} \right] \left[1 + \frac{4\pi P(r)r^3}{c^2 \mathcal{M}(r)} \right] \\ & \times \left[1 - \frac{2GM(r)}{c^2 r} \right]^{-1}, \\ d\mathcal{M}(r) = & 4\pi r^2 \rho(r) dr. \end{aligned} \quad (23)$$

Eqs. (22) and (23) are integrated from the star center to its surface, with the star radius R given by $P(R) = 0$. Other boundary conditions are

$$\begin{aligned} \mathcal{M}(0) &= 0, \quad \rho(0) = \rho_c, \quad P(0) = P_c, \\ H(0) &= 0, \quad H'(0) = 0, \quad \mathcal{M}(R) = M. \end{aligned} \quad (24)$$

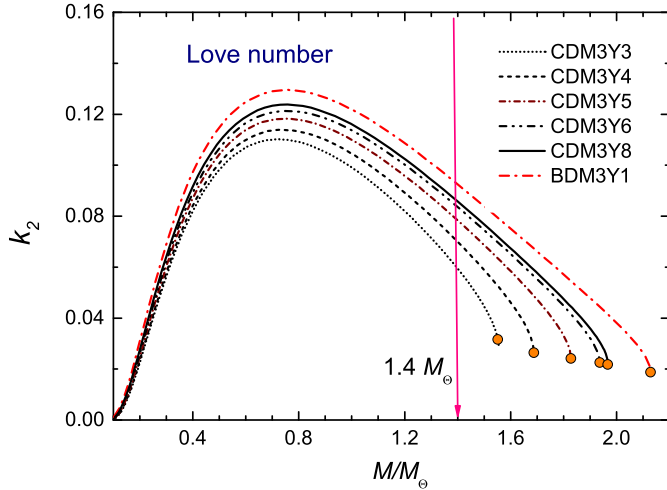


Fig. 5. The Love number (21) at different masses of NS given by the EOS of β -stable $npe\mu$ matter obtained with 6 versions of the density dependent NN interaction (2)-(4). The arrow crosses the k_2 values at $M = 1.4 M_\odot$, and the circles are those obtained at the corresponding maximum central densities n_c .

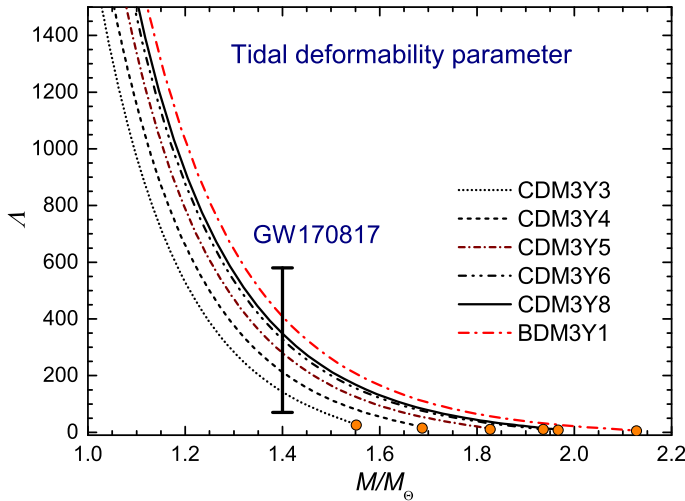


Fig. 6. The tidal deformability parameter (20) given by the EOS of β -stable $npe\mu$ matter obtained with 6 versions of the density dependent NN interaction (2)-(4). The vertical bar is the empirical tidal deformability at $M = 1.4 M_\odot$ inferred from the Bayesian analysis of the GW170817 data at the 90% confidence level [5], and the circles are λ values obtained at the corresponding maximum central densities n_c .

Our mean-field results (20)-(22) for the Love number and tidal deformability of NS are shown in Figs. 5 and 6, respectively. The k_2 number is reaching its maximum at $M \approx 0.7 \sim 0.8 M_\odot$, as found earlier by Hinderer *et al.* [2] using different EOS's of NS matter. With the increasing NS mass we observe a sizable difference between the k_2 values given by 6 versions of the density dependent NN interactions (2)-(4). Such a subtle effect is mainly due to the difference in the nuclear incompressibility K given by these interactions (see Table 2). For NS with mass $M = 1.4 M_\odot$, the larger the $R_{1.4}$ radius the larger the corresponding k_2 number. The tidal deformability of NS with mass up to above $2 M_\odot$ is shown in Fig. 6, and λ gradually decreases with the increasing NS mass, in a manner similar to that of the Love number shown in Fig. 5. The heavier the NS the smaller its tidal deformability, and the λ values given by 6 versions of the density dependent NN interaction for NS with $M = 1.4 M_\odot$ are all inside the empirical range implied by the GW170817 data at the 90% confidence level, $\Lambda_{1.4} \approx 190^{+390}_{-120}$ [5]. The impact by the nuclear incompressibility is significant: with K ranging from 217 to 270 MeV the corresponding $\Lambda_{1.4}$ value increases nearly by a factor of three (see Table 3).

From the macroscopic properties of NS given by the EOS of β -stable $npe\mu$ matter obtained with 6 versions of the interaction presented in Table 3 one can see a strong impact by the nuclear incompressibility K on the maximum gravitational mass M and radius R of NS. Namely, only the M values predicted by the CDM3Y6, CDM3Y8, and BDM3Y1 interactions (which are associated with $K = 252, 257,$ and 270 MeV, respectively) are close to the lower mass limit of the second PSR J0348 + 0432 ($M \approx 2.01 \pm 0.04 M_\odot$) [37] and the millisecond PSR J0740 + 6620 ($M \approx 2.14^{+0.20}_{-0.18} M_\odot$) [39]. The total pressure P of NS matter given by the CDM3Y6, CDM3Y8, and BDM3Y1 interactions at twice and six times the saturation density also agree well with the empirical pressure deduced from the GW170817 data at the 90% confidence level, $P(2n_0) \approx 3.5^{+2.7}_{-1.7} \times 10^{34}$ and $P(6n_0) \approx 9.0^{+7.9}_{-2.6} \times 10^{35}$ dyn/cm² [5]. The pressure given by the CDM3Y3 and CDM3Y4 interactions (associated with $K \approx 217$ and 228 MeV) becomes lower than the empirical pressure at high baryon densities $n_b > 3n_0$ as shown in Fig. 3. The difference in the K values also shows up in the calculated NS radius, and $R_{1.4} \approx 11.8$ and 12 km given by the EOS obtained with the CDM3Y8 and BDM3Y1 interactions, respectively, is about 1 km larger than those obtained with the CDM3Y3 and CDM3Y4 interactions (see Table 3 and Fig. 7). Excepting the results obtained with the CDM3Y3 interaction, the NS radii predicted by the EOS's obtained with other 5 versions of the density dependent NN interaction comply well with the empirical value of $R_{1.4} \approx 11.75^{+0.86}_{-0.81}$ km deduced recently from a joint analysis [10] of the two gravitational wave events GW170817 and GW190425, which originated from two different NS mergers.

Thus, the new constraints on the EOS of NS matter at high baryon densities [5,10] implied by the extra-terrestrial observations of the NS merger and the heaviest

Table 3. Properties of NS given by the EOS of β -stable $npe\mu$ matter obtained with 6 versions of the density dependent NN interaction (2)-(4). M and R are the maximum gravitational mass and radius of NS, respectively; n_c and P_c are the baryon number density and total pressure in the center of NS. $P(2n_0)$ and $P(6n_0)$ are the total pressure at twice and six times the saturation density, respectively. $R_{1.4}$, $k_{2(1.4)}$, $A_{1.4}$, and $C_{1.4}$ are the radius, Love number, tidal deformability parameter, and compactness of NS with $M = 1.4 M_\odot$, respectively.

EOS	M (M_\odot)	R (km)	n_c (fm^{-3})	$P_c/10^{35}$ (dyn/cm^2)	$P(2n_0)/10^{34}$ (dyn/cm^2)	$P(6n_0)/10^{35}$ (dyn/cm^2)	$R_{1.4}$ (km)	$k_{2(1.4)}$	$A_{1.4}$	$C_{1.4}$
CDM3Y3	1.55	9.3	1.53	8.9	2.9	3.7	10.6	0.059	142	0.194
CDM3Y4	1.69	9.6	1.43	9.6	3.2	4.6	11.2	0.070	212	0.186
CDM3Y5	1.83	9.9	1.32	10.1	3.5	5.6	11.5	0.078	280	0.180
CDM3Y6	1.94	10.1	1.22	10.3	3.8	6.8	11.7	0.084	327	0.176
CDM3Y8	1.97	10.1	1.21	10.7	3.8	7.2	11.8	0.086	348	0.175
BDM3Y1	2.12	10.4	1.11	11.8	4.2	9.6	12.0	0.092	407	0.172

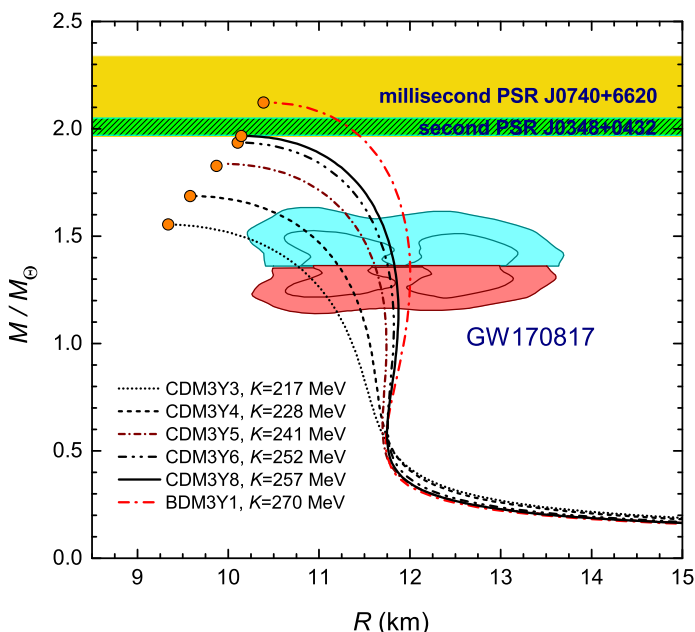


Fig. 7. The gravitational mass of NS versus its radius given by the EOS of β -stable $npe\mu$ matter obtained with 6 versions of the density dependent NN interaction (2)-(4). The GW170817 constraint for NS with mass $M = 1.4 M_\odot$ [5] is enclosed in the colored contours, and the circles are the M - R values calculated at the corresponding maximum central densities n_c . The shaded areas enclose the masses of the second PSR J0348+0432 [37] and millisecond PSR J0740 + 6620 [39], the heaviest neutron stars observed so far.

pulsars PSR J0348 + 0432 and PSR J0740 + 6620 can be used to probe the sensitivity of the EOS of NS matter to the nuclear incompressibility K . For the illustration, the NS mass versus its radius given by the EOS's of β -stable $npe\mu$ matter obtained with 6 versions of the density dependent NN interaction (2)-(4) is shown in Fig. 7. Like the Love number and tidal deformability of NS shown in Figs. 5 and 6, the M - R results obtained with 6 versions of the interaction comply well with the GW170817 constraint for NS with mass $M = 1.4 M_\odot$ [5] (the colored contours in Fig. 7). However, only the EOS's obtained with the CDM3Y6, CDM3Y8 and BDM3Y1 interactions

give the maximum mass M close to the observed lower mass limit of PSR J0348 + 0432 and PSR J0740 + 6620. It is interesting to note that the M - R curves obtained with 6 interactions seem to coincide at $M \approx 0.55 M_\odot$ and $R \approx 11.75$ km, and such a M - R point results from the behavior of the pressure of NS matter at the saturation density n_0 discussed in Fig. 3.

Although the impact of the nuclear incompressibility on the EOS of NM is well established [23, 24], much more efforts are made nowadays to explore the impact of the nuclear symmetry energy on the macroscopic properties of NS, like the sensitivity of the mass and radius of NS to the strength and slope of $E_{\text{sym}}(n_b)$ at high baryon densities [11, 31]. The results discussed in the present work remind us again of the important effect by the nuclear incompressibility K in the nuclear mean-field description of the EOS of NS matter. The results shown in Fig. 7 suggest that a stiffer EOS of NS matter associated with $K \approx 250 - 270$ MeV seems to comply better with the constraints implied by the gravitational wave observations of the NS merger and observed masses of the heaviest neutron stars. This result is complementary to the recent joint analysis of the NICER and LIGO/Virgo data [40], which prefers a stiff EOS associated with the masses of the heaviest pulsars observed so far.

It should be noted that the fast-rotating millisecond pulsar J0740 + 6620 might be associated with a strong magnetic field, so that the EOS of NS matter could also be affected by the spin polarization of baryons [41]. In particular, the maximum mass of magnetar might increase by about $0.1 M_\odot$ if 60 \sim 70% of baryons in NS matter are spin-polarized [19]. In such a scenario, the heavy mass ($M \approx 2.14^{+0.20}_{-0.18} M_\odot$) observed for the millisecond PSR J0740 + 6620 [39] could have imprints from both the spin polarization of baryons and incompressibility of NS matter. This should be the subject of further mean-field studies.

Summary

The EOS of asymmetric NM has been studied based on the nuclear mean-field potentials given by the nonrelativistic HF calculation using different versions of the density

dependent M3Y interaction that are associated with the nuclear incompressibility $K \approx 217 - 270$ MeV at the saturation density n_0 . From these scenarios of the EOS, only the CDM3Y6 and CDM3Y8 versions give the total energy of symmetric NM and pure neutron matter at high baryon densities close to the results of the ab-initio calculations of NM [20,21].

The HF mean-field potential is used to generate the EOS of β -stable $npe\mu$ matter, which is then compared with the empirical EOS (in terms of the total pressure of NS matter) deduced from the Bayesian analysis of the GW170817 data at the 90% confidence level [5]. We found that only the pressure of NS matter given by the EOS's obtained with the CDM3Y6, CDM3Y8, and BDM3Y1 interactions (associated with $K \approx 252, 257,$ and 270 MeV, respectively) agrees with the empirical pressure at high baryon densities, up to around $6n_0$.

The EOS of β -stable $npe\mu$ matter is also used to determine the tidal deformability Λ , mass M and radius R of NS using Eqs. (20)-(23) derived from the General Relativity. The obtained results show clearly the impact by the nuclear incompressibility K on the mean-field description of NS matter. While $\Lambda_{1.4}$ and $R_{1.4}$ given by all versions of the density dependent NN interaction are well inside the corresponding empirical ranges imposed for NS with mass $M = 1.4 M_\odot$ by the Bayesian analysis of the tidal wave signals from the NS merger GW170817 [5], only the EOS associated with $K \approx 250 - 270$ MeV gives the maximum gravitational mass of NS comparable to that deduced for the second PSR J0348 + 0432 and millisecond PSR J0740 + 6620, the heaviest neutron stars observed so far.

Acknowledgement We thank N. H. Phuc for his help in revising the isovector density dependence of the M3Y interaction. The present research was supported, in part, by the National Foundation for Science and Technology Development of Vietnam (NAFOSTED Project No. 103.04-2017.317).

References

1. T. Hinderer, *Astrophys. J.* **677**, 1216 (2008).
2. T. Hinderer, B. D. Lackey, R. N. Lang and J. S. Read, *Phys. Rev. D* **81**, 123016 (2010).
3. B. P. Abbott *et al.*, *Phys. Rev. Lett.* **119**, 161101 (2017).
4. B. P. Abbott *et al.*, *Astrophys. J. Lett.* **848**, L12 (2017).
5. B. P. Abbott *et al.*, *Phys. Rev. Lett.* **121**, 161101 (2018).
6. F. J. Fattoyev, J. Piekarewicz and C. J. Horowitz, *Phys. Rev. Lett.* **120**, 172702 (2018).
7. E. Annala, T. Gorda, A. Kurkela and A. Vuorinen, *Phys. Rev. Lett.* **120**, 172703 (2018).
8. S. De, D. Finstad, J. M. Lattimer, D. A. Brown, E. Berger and C. M. Biwer, *Phys. Rev. Lett.* **121**, 091102 (2018).
9. T. Malik, N. Alam, M. Fortin, C. Providência, B. K. Agrawal, T. K. Jha, B. Kumar and S. K. Patra, *Phys. Rev. C* **98**, 035804 (2018).
10. T. Dietrich, M. W. Coughlin, P. T. H. Pang, M. Bulla, J. Heinzel, L. Issa, I. Tews, and S. Antier, *Science* **370**, 1450 (2020).
11. D. T. Loan, N. H. Tan, D. T. Khoa and J. Margueron, *Phys. Rev. C* **83**, 065809 (2011).
12. N. H. Tan, D. T. Loan, D. T. Khoa and J. Margueron, *Phys. Rev. C* **93**, 035806 (2016).
13. N. Anantaraman, H. Toki and G. Bertsch, *Nucl. Phys. A* **398**, 269 (1983).
14. D. T. Khoa, G. R. Satchler and W. von Oertzen, *Phys. Rev. C* **56**, 954 (1997).
15. D. T. Khoa and G. R. Satchler, *Nucl. Phys. A* **668**, 3 (2000).
16. D. T. Khoa, W. von Oertzen and A. Ogloblin, *Nucl. Phys. A* **602**, 98 (1996).
17. D. T. Khoa, H. S. Than and D. C. Cuong, *Phys. Rev. C* **76**, 014603 (2007).
18. D. T. Khoa, B. M. Loc and D. N. Thang, *Eur. Phys. J. A* **50**: 34 (2014).
19. N. H. Tan, D. T. Khoa and D. T. Loan, *Phys. Rev. C* **102**, 045809 (2020).
20. A. Akmal, V. R. Pandharipande and D. G. Ravenhall, *Phys. Rev. C* **58**, 1804 (1998).
21. S. Gandolfi, A. Y. Illarionov, S. Fantoni, J. C. Miller, F. Pederiva and K. E. Schmidt, *Mon. Not. R. Astron. Soc. Lett.* **404**, L35 (2010).
22. U. Garg and G. Colò, *Prog. Part. Nucl. Phys.* **101**, 55 (2018).
23. Y. Schutz and TAPS Collaboration, *Nucl. Phys. A* **599**, 97c (1996).
24. D. T. Khoa, W. von Oertzen, H. G. Bohlen and S. Ohkubo, *J. Phys. G* **34**, R111 (2007).
25. M. B. Tsang, Z. Chajecki, D. Coupland, P. Danielewicz, F. Famiano, R. Hodges, M. Kilburn, F. Lu, W. G. Lynch, J. Winkelbauer, M. Youngs and Y. X. Zhang, *Prog. Part. Nucl. Phys.* **66**, 400 (2011).
26. A. Ono, P. Danielewicz, W. A. Friedman, W. G. Lynch and M. B. Tsang, *Phys. Rev. C* **68**, 051601 (2003).
27. L. Trippa, G. Colò and E. Vigezzi, *Phys. Rev. C* **77**, 061304 (2008).
28. R. Furnstahl, *Nucl. Phys. A* **706**, 85 (2002).
29. J. M. Dong, L. J. Wang, W. Zuo, and J. Z. Gu, *Phys. Rev. C* **97**, 034318 (2018).
30. X. H. Fan, J. M. Dong, and W. Zuo, *Phys. Rev. C* **89**, 017305 (2014).
31. W. J. Xie and B. A. Li, *Astrophys. J.* **883**, 174 (2019).
32. F. Douchin, P. Haensel and J. Meyer, *Nucl. Phys. A* **665**, 419 (2000).
33. F. Douchin and P. Haensel, *Astron. Astrophys.* **380**, 151 (2001).
34. E. Chabanat, P. Bonche, P. Haensel, J. Meyer and R. Schaeffer, *Nucl. Phys. A* **635**, 231 (1998).
35. S. L. Shapiro and S. A. Teukolsky, *Black Holes, White Dwarfs, and Neutron Stars* (WILEY-VCH Verlag GmbH & Co. KGaA, Weinheim, 2004), p.24.
36. I. Bombaci, in *Isospin Physics in Heavy Ion Collisions at Intermediate Energies*, edited by B. A. Li and W. U. Schröder (Nova Science, New York, 2001), p. 35.
37. J. Antoniadis *et al.*, *Science* **340**, 6131 (2013).
38. P. Bedaque and A. W. Steiner, *Phys. Rev. Lett* **114**, 031103 (2015).
39. H. T. Cromartie *et al.*, *Nat. Astron.* **4**, 72 (2020).
40. G. Raaijmakers *et al.*, *Astrophys. J. Lett.* **893**, L21 (2020).
41. J. M. Lattimer and M. Prakash, *Phys. Rep.* **442**, 109 (2007).